Phys. Status Solidi RRL **5**, No. 2, 80–82 (2011) / **DOI** 10.1002/pssr.201004488

pss +++rapid research letters+++
www.pss-rapid.com

Lateral IBIC characterization of single crystal synthetic diamond detectors

Alessandro Lo Giudice[1], Paolo Olivero[*, 1], Claudio Manfredotti[1], Marco Marinelli[2], Enrico Milani[2], Federico Picollo[1], Giuseppe Prestopino[2], Alessandro Re[1], Valentino Rigato[3], Claudio Verona[2], Gianluca Verona-Rinati[2], and Ettore Vittone[1]

[1] Experimental Physics Department – NIS Centre of Excellence, University of Torino and INFN – sez. Torino, via P. Giuria 1, 10125 Torino, Italy
[2] Dipartimento di Ingegneria Meccanica, Università di Roma "Tor Vergata", Via del Politecnico 1, 00133 Roma, Italy
[3] INFN- National Laboratories of Legnaro, Viale dell'Università 2, 35020 Legnaro (Pd), Italy

Received 16 November 2010, revised 5 January 2011, accepted 6 January 2011
Published online 11 January 2011

Keywords single crystals, diamond, ion beam induced charge, charge transport, detectors

[*] Corresponding author: e-mail olivero@to.infn.it, Phone: +39 011 670 7879, Fax: +39 011 669 1104

In order to evaluate the charge collection efficiency (CCE) profile of single-crystal diamond devices based on a p-type/intrinsic/metal configuration, a lateral Ion Beam Induced Charge (IBIC) analysis was performed over their cleaved cross sections using a 2 MeV proton microbeam. CCE profiles in the depth direction were extracted from the cross-sectional maps at variable bias voltage. IBIC spectra relevant to the depletion region extending beneath the frontal Schottky electrode show a 100% CCE, with a spectral resolution of about 1.5%. The dependence of the width of the high efficiency region from applied bias voltage allows the constant residual doping concentration of the active region to be evaluated. The region where the electric field is absent shows an exponentially decreasing CCE profile, from which it is possible to estimate the diffusion length of the minority carriers by means of a drift–diffusion model.

© 2011 WILEY-VCH Verlag GmbH & Co. KGaA, Weinheim

1 Introduction Diamond has extreme electronic and optical properties. The low intrinsic conductivity due to the wide bandgap, the high carrier mobility, the high thermal conductivity, the chemical inertness and the radiation hardness make it a good candidate as particle, UV and X-ray detector in many fields, especially in high radiation environments [1–4]. Although good results were obtained in the past using natural, high pressure high temperature (HPHT) and chemical vapor deposition (CVD) polycrystalline diamond, the last decade witnessed a vast improvement in the diamond detectors performances due to the development of homoepitaxial diamond (single crystal, SC) growth [5]. This material is characterized by high purity and low defect concentration, it exhibits long charge carrier lifetimes, high mobility and does not require a priming procedure before operation [6–8]. Recent results obtained in the detection of UV light [9], X-rays [10] and neutrons [11] with SC-diamond detectors are very promising.

Ion beam induced charge (IBIC) is a very suitable technique to characterise transport properties in wide band gap semiconductors employed as ionizing radiation detectors [12]. SC-diamond detectors were already studied by means of frontal IBIC [13]. In this Letter we report on the characterization of diamond SC Shottky diodes by means of lateral IBIC technique.

2 Experimental The device was developed starting from a single-crystal diamond grown by CVD technique at the laboratories of Rome "Tor Vergata" University. Diamond was grown on a HPHT substrate in a p-type/intrinsic layered structure by a two-step plasma-enhanced microwave CVD homoepitaxial deposition process. A cross-sectional schematic of the device is reported in Fig. 1. A commercial HPHT Ib single crystal diamond $4 \times 4 \times 0.4$ mm^3 in size was used as substrate. A ~ 20 μm thick heavily boron-doped (~10^{20} cm^{-3}) layer was first deposited on the HPHT substrate followed by the deposition of a 30 μm thick diamond layer with a net electrically active acceptor-like defect concentration of the order of 10^{14} cm^{-3} [10]. A circular Al contact with a diameter of 2 mm and 200 nm

© 2011 WILEY-VCH Verlag GmbH & Co. KGaA, Weinheim

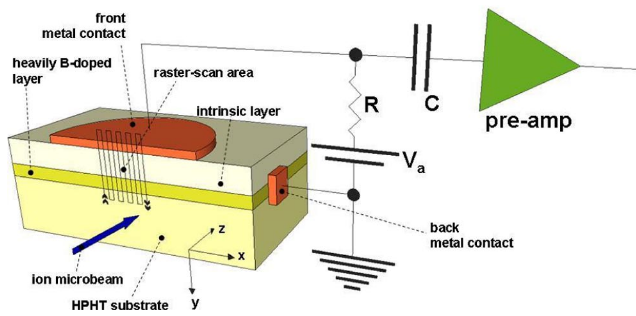

Figure 1 (online colour at: www.pss-rapid.com) Schematics of the diamond detector cross-sectional structure, connection to the acquisition electronic chain, and ion beam probe geometry. The drawing is not to scale.

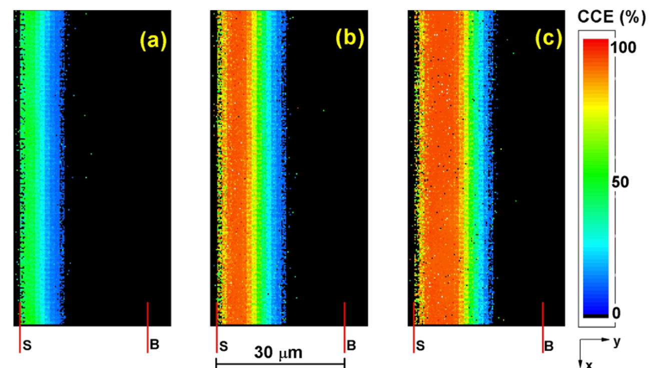

Figure 2 (online colour at: www.pss-rapid.com) Lateral IBIC maps relevant to bias voltages: a) 0 V, b) 25 V, c) 60 V. The vertical lines at the bottom of the maps indicate the position of the Schottky (S) frontal sensitive electrode and of the B doped back electrode (B).

thick was then deposited on the intrinsic diamond surface, while annealed ohmic silver back electrodes were formed on the heavily B-doped layer (see Fig. 1). The sample was cleaved in order to expose the cross section to the ion beam irradiation and edge-on mounted to perform lateral IBIC experiments.

IBIC measurements were carried out at the AN2000 microbeam facility of the National Laboratories of Legnaro (Italy) by using 2 MeV protons. The beam was focused to a spot size of ~2 μm and raster-scanned over the cleaved cross section of the diamond sample from the Schottky contact to the highly doped substrate ($62 \times 62\ \mu m^2$ scan area), as schematically shown in Fig. 1.

As evaluated by the SRIM Monte Carlo Simulation code [14], the range of 2 MeV protons in diamond is about 25 μm, while their lateral straggling is ~0.66 μm. Since the electron/hole generation occurs primarily at the Bragg's peak, it is reasonable to assume negligible charge or recombination effects at the irradiated cross-section surface. As a consequence, the induced charge signals collected at the sensitive frontal electrode can be considered as due to the motion of free carriers generated in the bulk of the diamond sample, and subjected to an electric field oriented orthogonally to the two electrodes.

The system provided a spectral sensitivity of 270 electrons/channel and a spectral resolution (defined as the FWHM of the 2 MeV proton peak in the Si surface-barrier detector used as reference) of about 3900 electrons, corresponding to an energy resolution of 14 keV in silicon.

3 Results and discussion Room temperature current–voltage (I–V) characterization in reverse and forward polarizations yielded a good rectification effect due to the presence of a Schottky barrier at the Al electrode, whereas the highly doped back contact is assumed to be ohmic.

The linear behaviour of the I–V curve in reverse polarization for $V < -20$ V indicated the presence of a shunt resistance $R_{sh} = (900 \pm 6)$ GΩ. From the forward bias behaviour an ideality factor $n = (1.51 \pm 0.04)$, a series resistance $R_s = (5.1 \pm 1.6)$ kΩ and a saturation reverse current of $(1.0 \pm 0.6) \cdot 10^{-23}$ A were derived. The high value of R_s is probably due to the highly B-doped electrode at the bottom of the active region. Assuming an effective Richardson constant of 92 A cm^{-2} K^{-2} [15], the barrier height can be estimated around 1.4 eV.

Figure 2 shows lateral IBIC maps at different reverse bias voltages. The CCE is encoded in colour scale, being derived from the median of the IBIC pulse distribution for each pixel. The highest charge is induced by the motion of carriers generated in the proximity of the Schottky electrode, which roughly corresponds to the depletion region where a strong electric field occurs. At zero bias, the maximum induced charge occurs in a region extending around 5 μm beneath the Schottky barrier; as the applied bias increases, the extension of the high efficiency IBIC region widens.

In Fig. 3a the CCE profiles obtained by projecting the CCE maps along the y-axis are reported. These profiles exhibit the same behavior observed in previously analyzed partially depleted silicon p–n junctions [16] and Schottky diodes [17], which have been interpreted using the drift–diffusion model for charge induction based on the Shockley–Ramo–Gunn theorem [12].

In a simplified version of this model, charge pulses are formed only in regions where an electric field (E) is present, i.e. within the depletion region W, and the amount of the induced charge is proportional to the d/W ratio, where $d = \mu \cdot \tau \cdot E$ is the carrier drift length and $\mu \cdot \tau$ is the mobility (μ)–lifetime (τ) product. Due to the fast drift, no recombination occurs during the time of flight of electron and holes throughout the thickness W, and the induced charge is equal to the generation charge (i.e. CCE = 100%) for carriers generated within the depletion region, which widens as the applied bias voltage increases. Moreover, the dependence of the extension of the depletion region W from the applied voltage V_a can be interpolated with the well known formula:

$$W = \sqrt{2 \cdot \varepsilon_r \cdot \varepsilon_0 \cdot (V_a + V_{bi})/(e \cdot N_A)} \qquad (1)$$

© 2011 WILEY-VCH Verlag GmbH & Co. KGaA, Weinheim

physica status solidi rrl

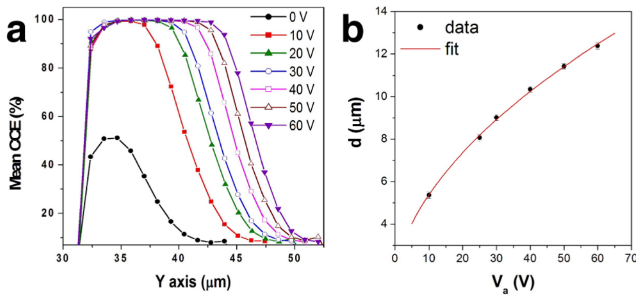

Figure 3 (online colour at: www.pss-rapid.com) (a) CCE profiles at different bias voltages. (b) Plot of the extension of the depletion region as evaluated from the IBIC maps as a function of applied bias voltage.

where ε_r and ε_0 are the relative and vacuum dielectric constants, e is the elementary electrical charge, N_A is the net electrically active acceptor-like defect concentration and V_{bi} is the built-in potential at the Schottky barrier. As shown in Fig. 3b, the experimental data are satisfactorily fitted by this trend, yielding a value of the built-in voltage of (1.3 ± 0.8) V, to be compared with the value (1.4 V) obtained by $C-V$ measurement, and an estimation of the net electrically active acceptor-like defect concentration of $N_A = (2.43 \pm 0.13) \times 10^{14}$ cm^{-3}, in good agreement with previous estimations [10].

On the other hand, for $y > W$, i.e. in the region where no electric field is present, electrons and holes diffuse away from the generation point. The charge at the sensing electrode is induced only by the motion of free carriers in presence of the applied electric field, so no induction occurs from their motion in the neutral region [12]. However, their thermal random motion produces a diffusion current towards the depleted region. While majority carriers (holes) are driven back by the electric field, the minority carriers (electrons) penetrate this region, are drifted towards the sensitive electrode, and induce a current proportional to their flux. Being diffusion a much slower transport mechanism, recombination effects attenuate the population of electrons entering the active region. As the distance of the generation point from the depletion region increases, assuming an homogeneous material throughout the entire epitaxial layer, the probability of electrons to enter the depletion region exponentially decreases, with a logarithmic slope equal to their diffusion length $L_e = (D_e \cdot \tau_e)^{1/2}$, where D_e and τ_e are the electron diffusivity and lifetime, respectively. The fit procedure of the exponentially decreasing tails reported in Fig. 3a provides an average electron diffusion length of $L_e = (2.6 \pm 0.2)$ μm, in excellent agreement with the value reported in [10]. Using the Einstein relation for the diffusivity/mobility ratio, the product of the zero field mobility (μ_e) and the lifetime is evaluated as $\mu_e \cdot \tau_e = (2.5 \pm 0.3) \times 10^{-6}$ V cm^{-2}, a value which is in good agreement with what reported in [6, 18], providing an electron lifetime estimate of ~1 ns, if a mobility of the order of 2000 cm^2 V^{-1} s^{-1} is considered [19, 20].

4 Conclusions Lateral IBIC characterization was employed to characterize the charge transport properties of SC diamond devices. In the active region, the device yielded a 100% efficiency with a spectral resolution of about 35 keV. The variation of the width of the depletion region as function of the applied bias voltage allows the estimation of the acceptor-like defect concentration in the nominally intrinsic layer to a value of $(2.43 \pm 0.13) \times 10^{14}$ cm^{-3}. The analysis of the tails of the CCE profiles provides a value of the mobility–lifetime product for electrons of 2.5×10^{-6} cm^2 V^{-1}, which corresponds to an average lifetime of the order of ~1 ns if typical mobility values are assumed.

Acknowledgements This work was supported in the framework of the INFN experiment DIARAD and MiUR-PRIN2008 National Project "Synthetic single crystal diamond dosimeters for application in clinical radiotherapy". The work of P. Olivero was supported by the "Accademia Nazionale dei Lincei – Compagnia di San Paolo" Nanotechnology grant.

References

[1] A. Paoletti and A. Tucciarone (Eds.), The Physics of Diamond (OS Press, Amsterdam, 1997).
[2] J. H. Kaneko et al., Nucl. Instrum. Methods Phys. Res. A **505**, 187 (2003).
[3] W. Adam et al., Nucl. Instrum. Methods Phys. Res. A **565**, 278 (2006).
[4] D. Tromson et al., Diam. Relat. Mater. **19**, 1012 (2010).
[5] J. Isberg et al., Science **297**, 1670 (2002).
[6] J. Isberg et al., Diam. Relat. Mater. **13**, 872 (2004).
[7] M. Pomorski et al., Diam. Relat. Mater. **16**, 1066 (2007).
[8] N. Nesladek, Diam. Relat. Mater, **17**, 1235 (2008).
[9] S. Almaviva et al., Diam. Relat. Mater. **19**, 78 (2010).
[10] S. Almaviva et al., J. Appl. Phys. **107**, 014511 (2010).
[11] S. Almaviva et al., Nucl. Instrum. Methods Phys. Res. A **612**, 580 (2010).
[12] M. B. H. Breese et al., Nucl. Instrum. Methods Phys. Res. B **264**, 345 (2007).
[13] C. Manfredotti et al., Diam. Relat. Mater. **16**, 940 (2007).
[14] J. F. Ziegler, J. P. Biersack, and M. D. Ziegler, SRIM – The Stopping and Range of Ions in Matter (Ion Implantation Press, 2008).
[15] R. Kumaresan et al., Diam. Relat. Mater. **19**, 1324 (2010).
[16] C. Manfredotti et al., Nucl. Instrum. Methods Phys. Res. B **158**, 476 (1999).
[17] P. Olivero et al., accepted for publication in Nucl. Instrum. Methods Phys. Res. B (2010).
[18] A. Lohstroh et al., Appl. Phys. Lett. **90**, 102111 (2007).
[19] L. S. Pan and D. R. Kania, Diamond: Electronic Properties and Applications (Kluwer Academic Publishers, Boston–Dordrecht–London, 1993).
[20] M. Marinelli et al., Appl. Phys. Lett. **89**, 143509 (2006).

© 2011 WILEY-VCH Verlag GmbH & Co. KGaA, Weinheim